

Modeling of the cylinder liner “zero-wear” process by two-scale homogenization technique



Xianghui Meng ^{a,b,*}, Yang Hu ^{a,b}, Youbai Xie ^{a,b}

^a State Key Laboratory of Mechanical System and Vibration, Shanghai Jiaotong University, Shanghai 200240, People's Republic of China

^b School of Mechanical Engineering, Shanghai Jiaotong University, Shanghai 200240, People's Republic of China

ARTICLE INFO

Article history:

Received 18 July 2016

Received in revised form

14 October 2016

Accepted 19 October 2016

Available online 21 October 2016

Keywords:

“Zero-wear”

Two-scale

Homogenization technique

Mixed lubrication

Cylinder liner

Wear modeling

ABSTRACT

“Zero-wear” is considered as wear within the limits of surface topography of the component. The honed cylinder liner surface is composed of the plateaus and relatively deep valleys. In this paper, a two-scale homogenized mixed lubrication and wear model is established to study the “zero-wear” process of the cylinder liner. In order to consider the plateau roughness and the valleys separately on local and global scales, the honed surface is firstly decomposed into plateaus and valleys by the morphological filtering approach. Then, based on two-scale homogenization technique, a homogenized mixed model is developed to characterize the lubrication properties and the contact severity of the piston ring-liner system. On this basis, the cylinder liner “zero-wear” process is divided into two stages: at the first stage, running-in of the plateau component on the local scale; at the second stage, wear of the valley component on the global scale. On the local scale, the influence of the plateau component running-in on the homogenized flow factors and contact stiffness is studied. On the global scale, the influence of the valley component wear on the lubrication properties (load carrying capacity, contact force and friction coefficient) is studied. Experiments are conducted on a reciprocating tester. The experimentally measured friction coefficient and wear depth are shown to be in good agreement with the simulation results. The results showed that the two-scale homogenized mixed lubrication and wear model developed in this paper can well predict the cylinder liner “zero wear” process.

© 2016 Elsevier B.V. All rights reserved.

1. Introduction

The cylinder liner surface topography is an important factor that affects the friction, wear and lubrication of the piston ring-liner system. During the operation of an internal combustion engine, the cylinder liner surface topography is constantly changing due to wear. The wear of surface topography is generally referred to as “zero-wear”, for which the wear volume or amount is within the limits of the original surface topography [1,2]. The wear of the cylinder liner surface topography will not only change the tribological properties of the piston ring-liner system, but also may lead to the scuffing of the cylinder bore [3]. Therefore, it is of great significance to study the “zero-wear” process of the cylinder liner.

The cylinder liner is usually produced by the honing process. The final honed cylinder liner surface is composed of the plateaus and the valley components. The plateau roughness and the groove

parameters of the valley component will change during the cylinder liner “zero-wear” process. These changes will affect the mixed lubrication properties of the piston ring-liner system, and the lubrication behavior will in turn affect the wear process of the cylinder liner surface topography. Therefore, when simulating the “zero-wear” process of the cylinder liner, it is necessary to consider the mutual dependency of mixed lubrication and wear. Scholars have done a lot of research work on mixed lubrication simulation and wear prediction.

Based on real measured surface topography, Hu and Zhu [4] have developed a full-scale deterministic mixed lubrication model, which solve both hydrodynamic lubrication and surface contact, simultaneously. The model can predict the distributions of hydrodynamic pressure, film thickness, and asperity deformation, etc., as functions of location and time. On this basis, Zhu Dong et al. [5] have integrated the wear on surface topography into the model, taking into account the mutual dependency of wear and lubrication. However, this deterministic simulation method is limited to the point contact and other issues with small computing area. When applied to the friction pairs in actual engineering, the calculation cost is too high to be acceptable.

* Correspondence to: State Key Laboratory of Mechanical System and Vibration, School of Mechanical Engineering, Shanghai Jiaotong University, Shanghai 200240, People's Republic of China.

E-mail addresses: xhmeng@sjtu.edu.cn (X. Meng), huyang0330@126.com (Y. Hu).

Nomenclature

a	one-dimensional homogenized flow factor	$P(M)$	the plateau roughness
b	one-dimensional homogenized flow factor	$R(M)$	the reference surface or the waviness or form elements
F_T	the applied load (N)	s	the sliding distance (m)
g	the global scale subscript	S_j	the node on the stroke
h	the wear depth (m)	S	the coordinate along the sliding direction at the center of the stroke
h_d	the depth of the groove (m)	t	the slow time scale
h_g	the wear depth on the global scale (m)	U	the speed of moving surface (m/s)
h_l	the wear depth on the local scale (m)	Vol	the worn volume (m^3)
h_T	the groove description (m)	$V(M)$	the valley component
\bar{h}	the average film thickness at a given separation (m)	w_0	using to adjust the width of the honing groove
H	the hardness of the soft material (Pa)	W	the ring width (m)
$I(M)$	the measured surface profile	x	the global scale coordinate at the center of the piston ring
k	the dimensional wear coefficient (Pa^{-1})	x_0	the position of the honing groove
k_g	the dimensional wear coefficient on the global scale (Pa^{-1})	y	the local scale coordinate
k_l	the dimensional wear coefficient on the local scale (Pa^{-1})	y_j	the node on the plateau
K	the dimensionless wear coefficient	δh_g	the wear depth increment over one cycle on the global scale (m)
l	the local scale subscript	δh_l	the wear depth increment over one cycle on the local scale (m)
L	the length of roughness measurement (m)	Δh	the wear depth increment (m)
M	the sampling point	Δs	the sliding distance increment (m)
p_c	the contact pressure (Pa)	Δt_g	the time step of wear calculation on the global scale (s)
p_{cg}	the contact pressure variation with time over one cycle on the global scale (Pa)	Δt_l	the time step of wear calculation on the local scale (s)
p_{cl}	the asperity contact pressure distribution on the local scale (Pa)	$\Delta \tau$	the time interval of one cycle (s)
p_0	the homogenized pressure solution (Pa)	η	the lubricant viscosity (Pa s)
$\overline{p_c}$	the average contact pressure (Pa)	ρ	the lubricant density (Kg m^{-3})
		τ	the fast time scale

In order to accelerate the calculation, it is necessary to use an average method to consider the influence of surface roughness. Most of the existing models [6,7] in the simulation of the piston ring-liner system mixed lubrication, adopted the Patir and Cheng's average flow method [8] to consider the influence of surface roughness on fluid lubrication. The Patir and Cheng's method assumed that the cylinder liner surface topography is subject to the Gaussian distribution. Moreover, the effects of plateau roughness and cross-hatched textures were considered in the same set of flow factors by this method. The asperity contact was usually calculated by using the Greenwood-Williamson or Greenwood-Tripp model [9,10]. Although this method is fast, it has three shortcomings. Firstly, it is difficult to quantitatively determine the statistical parameters. Secondly, the real cylinder liner surface is generally not subject to Gaussian distribution. This assumption of Gaussian distribution will result in errors. The surface topography will further deviate from the Gauss distribution assumption during the "zero-wear" process. Thirdly, the cylinder liner wear will lead to the disappearance of local surface textures, which will influence the local lubrication effectiveness and even lead to the scuffing of the liner. However, in the Patir and Cheng's method, the effects of plateau roughness and the honed surface texture were considered in the same set of flow factors, which is not beneficial for the prediction of "zero-wear" of cylinder liner.

In recent years, the proposed two-scale homogenization technique provides a new way for solving the mixed lubrication problem between the rough surfaces [11,12]. In the homogenization procedure, the surface roughness on the local scale, which can be expressed using a periodic function, is decoupled from the smooth geometry on the global scale. As shown in Fig. 1(a), the oil film thickness is modeled by one part describing the geometry of the

piston ring-liner contact and the other periodic part describing the surface roughness. Fig. 1(b) shows a series of the deterministic solutions with different roughness wavelength and the corresponding homogenized solution. It can be seen that the homogenized approximation of the deterministic solution becomes more accurate when the roughness wavelength of the deterministic solution becomes smaller. Actually, the homogenized solution describes the limiting result when the wavelength of the surface roughness goes to zero by using the deterministic solution. Based on this conclusion, Sahlin et al. [13,14] proposed a homogenized mixed lubrication model. By using a measured topography of a part of the surface as input, the homogenized flow factors are calculated to consider the influence of surface roughness on lubrication. The contact stiffness is calculated by a deterministic asperity contact model considering the elastic plastic deformation. By using the real measured topography as input, the proposed model may be more accurate than the average flow model with the statistical parameters as input. In addition, this model is more suitable for non-Gaussian distribution engineering surface, such as the honed cylinder liner surface. Furthermore, compared with the deterministic mixed lubrication model [4], the homogenized mixed lubrication model can reduce the computation time greatly but ensure the accuracy [15]. To guarantee the accuracy of the homogenization approach, it is necessary to ensure that the local scale feature is small enough relative to the global scale. Spencer et al. [16] applied the homogenized method to the study of the piston ring-liner system. They found that an unacceptable error will result from treating the plateau roughness and the honed texture both on the local scale. So it is suggested that the effects of the honed texture should be considered on the global scale to ensure high accuracy.

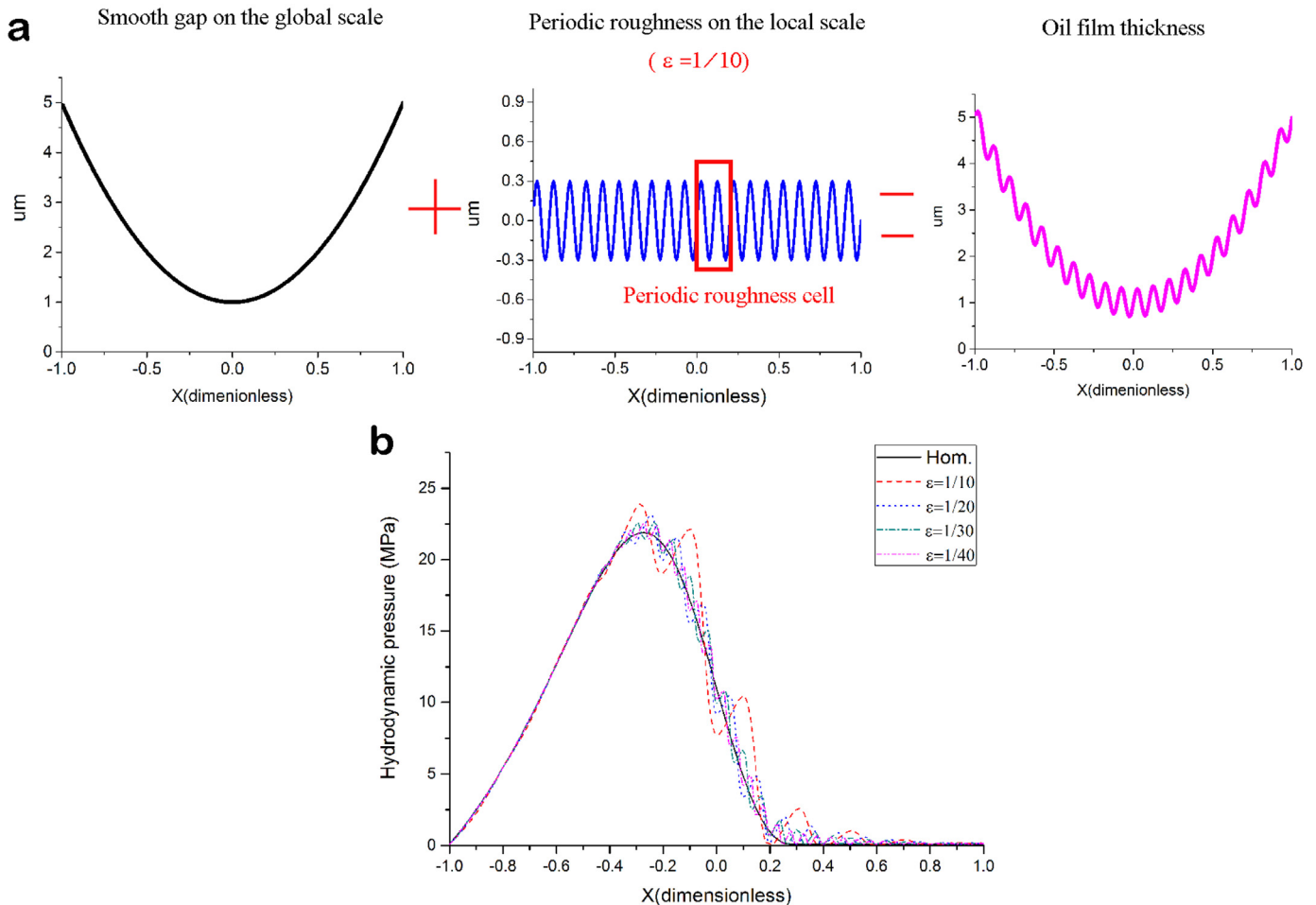


Fig. 1. (a) oil film thickness description; (b) a series of the deterministic solutions and the corresponding homogenized solution, note: the periodic roughness is defined as $h_r = 0.3 \sin(2\pi X/\epsilon)$ and ϵ is the wavelength of surface roughness.

On the aspect of developing wear model to predict the wear process, researchers have also done a lot of work. One of the earliest works in predicting wear was conducted by Archard [17]. Furthermore, the Archard model is now the most widely used wear model. The general methodology of simulating the wear process is to firstly solve the contact problem in order to determine the contact stress, and then calculate the amount of wear based on the wear model, and update the geometric profile according to a certain time step [18]. In recent years, the contact problems have been solved by using the finite element method [19,20], the boundary element method [21,22], and the deterministic Fast Fourier Transform (FFT)-accelerated contact model [23]. Based on solving the contact problem, the change of surface topography and geometrical profile can be predicted by wear calculation. For example, Furustig et al.[24] simulated the evolution of the surface topography and the geometric profile of the hydraulic motor based on the Archard wear model.

In this paper, a two-scale homogenized mixed lubrication and wear model is established to study the cylinder liner “zero-wear” process. Firstly, the lubrication properties and the contact severity of the piston ring-liner system are accurately evaluated by using the homogenized mixed lubrication model. Then, based on the Archard wear model, the “zero-wear” of the cylinder liner is quantitatively investigated on two scales: on the local scale, considering the superficial plateau wear; and on the global scale, considering the valley component wear. In this study, the real measured surface topography of a part of the cylinder liner is used as input to the

model. The mutual dependency of surface topography wear and mixed lubrication are considered in the simulation of the cylinder liner “zero-wear” process. Finally, the developed model will be verified by experiments. It should be noted that this study focuses on the “zero-wear” process of the cylinder liner. It is assumed that the piston ring is smooth, and the influence of ring wear on the wear process of the cylinder surface topography is ignored.

2. Two-scale homogenized mixed lubrication and wear model

2.1. Statement of the problem and assumptions

The piston ring-liner system in an internal combustion engine is a friction pair of reciprocating motion. To facilitate the experimental verification, liner samples are tested against the piston ring samples on a reciprocating tester as shown in Fig. 2. The running conditions used in the tests is to replicate the conditions around the top-dead center (TDC) of an engine. In this study, the numerical model will be developed to reflect the experiments. The specific details of the experiments can be seen in Section 3.

For the wear process shown in Fig. 2, the following assumptions and treatments are made before the construction of the two-scale wear model.

- (1) It is expected that during the cylinder “zero-wear” process, the plateaus become smooth firstly, and then the large valleys are

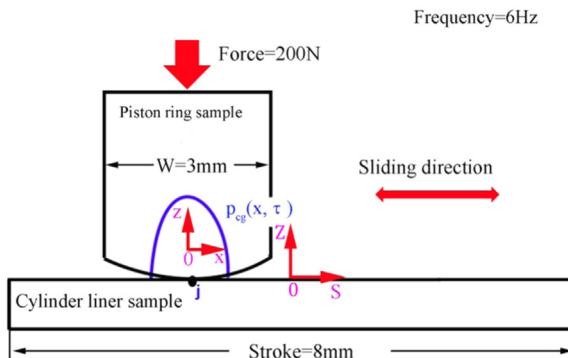


Fig. 2. Schematic diagram of the piston ring-liner reciprocating test.

transformed into many small valleys. Therefore, in this study, the cylinder “zero-wear” process is divided into two stages. At the first stage, the superficial plateau roughness decreases to a stable value rapidly due to the wear of the superficial plateau asperities. At the second stage, the valley depth is decreased due to the wear of the valley component. It is assumed that the plateau roughness at the second stage is the stable value of the first stage after running-in, and remains unchanged. Wear calculations on these two scales are based on the Archard wear model. In the following description, the subscript l is used to represent the local scale, and the subscript g is used to represent the global scale.

- (2) In case of the plateau wear on the local scale, it is assumed that the contact severity at different locations on the stroke is the same when the piston ring is passing by within one cycle. In this way, the wear process of the plateau component within the entire stroke can be reflected by simulating the wear process of a part of the plateau component with length of 1 mm along the sliding direction. The reasons are as follows. On one hand, the reciprocating stroke of 8 mm is very short compared with the ring width of 3 mm. On the other hand, the load remains constant and is very large due to that the running conditions used in the tests is to replicate the conditions around the TDC of an engine. As a result, the contact severity of the plateau component at different positions of the stroke is nearly the same. Moreover, during the running-in of the plateau component, the running-in time is very short within several minutes, and the wear amount is very small. Therefore, this simplified treatment is reasonable and is convenient for wear simulation. However, when simulating the cylinder “zero-wear” in an internal combustion engine, this simplified treatment will bring unacceptable errors due to the fact that the actual stroke is much longer, and the load at different positions of the stroke varies a lot. In this case, the stroke should be segmented to consider the contact severity differences at different positions of the stroke.
- (3) In case of the valley component wear on the global scale, the differences of groove parameters and contact severity at different positions of the stroke are considered.
- (4) According to the literatures [18], the wear process is usually slower compared with the mixed lubrication problem. Therefore, the mixed lubrication problem and the wear process can be partially decoupled. Two time scales can be introduced: the slow time is related to the profile evolution due to wear; the fast time corresponds to one cycle of reciprocating motion referring to the reciprocating test. In this paper, the fast time scale τ is used to calculate the mixed lubrication problem; the slow time scale t is used to calculate the wear evolution.

2.2. Morphological decomposition of a honed cylinder liner surface

The honed cylinder liner surface is composed of superficial plateau roughness separated by relatively deep valleys. These two elements play different roles in the piston ring-liner system [25]. The plateau roughness is related to friction and wear; and the valley component is related to lubrication and reservoirs.

In the homogenized mixed lubrication and wear model, the plateau roughness and valley component are taken into consideration in separate scales, thus, decomposing of an engine bore finish surface into plateau roughness and the valleys is necessary. The morphological filtering approach provides a powerful tool as described in [25]. An example of decomposition of the honed surface is shown in Fig. 3. Fig. 3(a) shows a 2D surface profile measured by a stylus measuring device. For 2D profiles, this approach uses an alternate sequential filter, with a linear structuring element, as non-linear image processing operator. When an alternate sequential filter of size n with a linear structuring element E is applied to the acquired surface ' I ', all peaks and valleys smaller than $n \times E$ are erased from the surface. $n \times E$ should be larger than the largest valley or roughness element, but smaller than waviness or form elements, then the output reference surface ' R ' will correspond to the waviness or form elements, as shown in Fig. 3(b). The elementary structuring element E and the maximum filtering size n are two important parameters in the decomposition procedure. For 2D profiles, the smallest linear structuring element has been chosen in a digital grid of 1×3 . For the honed surface of the cylinder liner, the largest valleys are around $50 \mu\text{m}$ wide. For the stylus measuring equipment used, the sampling step is $0.5 \mu\text{m}$. Here, the value of n has been set equal to 100. Therefore the largest topography elements that have been erased are $2 \times 100 \times 0.5 = 100 \mu\text{m}$, which is far greater than the width of the largest valley, but smaller than its low frequency components. Plateau roughness ' P ' lies above the reference surface and the valleys ' V ' lie below the reference as shown in Fig. 3(c) and (d), respectively. If M is a sampling point then:

$$P(M) = \begin{cases} I(M) - R(M) & \text{if } I(M) > R(M) \\ 0 & \text{otherwise} \end{cases} \quad (1)$$

$$V(M) = \begin{cases} I(M) - R(M) & \text{if } I(M) < R(M) \\ 0 & \text{otherwise} \end{cases} \quad (2)$$

The separated plateau roughness will be used to calculate the homogenized flow factors and contact stiffness, thereby taking into account the influence of the plateau roughness on the lubrication properties of the piston ring-liner system. In order to consider the influence of the valley component (grooves) on the global scale, three non-standard parameters are introduced, including the average groove depth, the average groove width, and the average groove distance. These parameters have been successfully applied in the literatures [26–28]. The effect of honing angle is temporarily not considered. After obtaining these parameters, a single groove can be generated by using the follow equation [29]:

$$h_T(x) = h_d 10^{-w_0(x-x_0)^2} \cos(2\pi(x-x_0)) \quad (3)$$

The groove geometry is defined by three parameters:

- h_d depth of the groove,
- w_0 using to adjust the width of the honing groove,
- x_0 position of the honing groove.

The groove generated by Eq. (3) was repeated within the ring

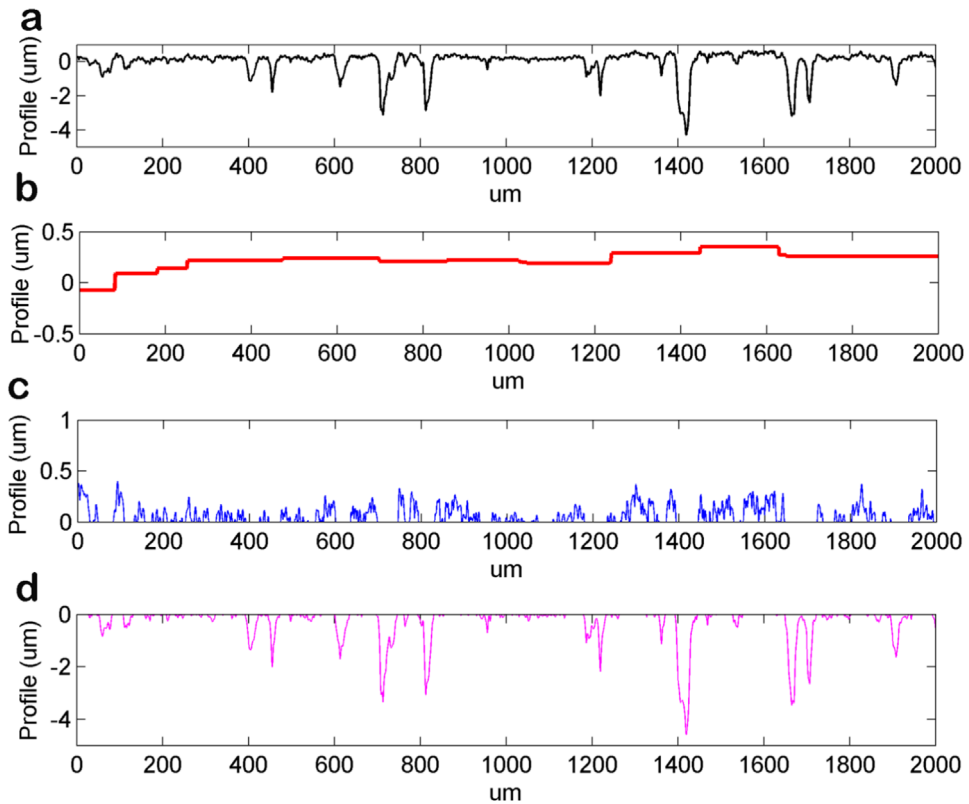


Fig. 3. (a) 2D surface profile I of a honed surface measured by a stylus measuring device; (b) the reference surface R or waviness or form elements; (c) plateau roughness P ; and (d) valley component V .

width along the sliding direction. The average groove depth, the average groove width, and the average groove distance of the valley component are 1.493 μm , 25 μm and 153 μm , respectively.

2.3. Homogenized mixed lubrication model

In this paper, the lubrication of piston ring-liner system is treated as a one-dimensional problem. Although the one-dimensional model cannot take into consideration the variation in the circumferential direction and the honing angle, its low computational effort and acceptable calculation precision are beneficial for the study of the cylinder “zero-wear” process [30,31]. A one-dimensional homogenized mixed lubrication model is used to consider the effects of the cylinder liner surface topography. In the model, the plateau roughness is considered on the local scale; the valley component is considered on the global scale. Differing from the Patir and Cheng's method, the real surface topography measured is used as the input to the model instead of the statistical parameters.

2.3.1. Homogenized Reynolds equation

In order to consider the influence of surface roughness on the lubrication flow, the one-dimensional homogenized Reynolds equation is used

$$\frac{\partial}{\partial x} \left(\rho a \frac{\partial p_0}{\partial x} \right) = 6\eta U \frac{\partial(\rho b)}{\partial x} + 12\rho\eta \frac{d\bar{h}}{dt} \quad (4)$$

where p_0 is the homogenized film pressure, \bar{h} is the average film thickness at a given separation, a and b are the homogenized flow factors.

Lubrication viscosity-pressure variation can be predicted using the Roelands equation [32]. While the density variation with the

pressure given by Dowson and Higginson [33] can be used for the prediction of lubricant's density.

Cavitation effects are taken into account in the Reynolds equation by means of the complementary Swift-Steiber (or Reynolds) boundary conditions [31]. This cavitation model is much easier to deal with numerically and has been successfully used in several publications to study the effects of surface textures [34,35], although, it does not satisfy the mass conservation of the lubricant flow throughout the cavitation boundaries.

2.3.2. Calculation of the homogenized flow factors and contact stiffness

Flow factors are functions of separation between a measured surface and a theoretical smooth opposing surface. They can be thought of as correction factors, which are used to modify the Reynolds equation to incorporate the averaged effect of surface roughness [36]. The plateau roughness decomposed from the honed cylinder liner will be used to calculate the homogenized flow factors. The evaluation length of the plateau roughness is a matter of concern. Typically, the longer the evaluation length, the more the roughness number, as a result, the calculation is more accurate. However, it is well known that the plateaus are separated into many small regions with size of about $150 \times 150 \mu\text{m}$ by the valleys. One of the advantages of decomposition of the cylinder liner surface by using the morphological filtering approach lies in that the evaluation length of the plateau roughness can be selected very long without the limit of the groove distance. It should be noted that the separated plateau roughness contains many regions without asperities where the valleys exist in these regions before decomposition. These regions must be abandoned before the calculation of the homogenized flow factors and contact stiffness. In this paper, the evaluation length of the plateau roughness is

chosen as 1 mm. In order to show more clearly, only a portion with length of 200 μm is shown in the following figures. The separated plateau roughness is also used as input to the contact model to obtain the contact stiffness. Detail information about the calculation process of the homogenized flow factors and contact mechanics model used is well described in references [13,14,36] and is not repeated here. Fig. 4 displays the deformed surface roughness profile and the corresponding asperity contact pressure distribution. The relationship between the mean contact pressure \bar{p}_c and the separation h_0 is called contact stiffness. In the contact mechanics model, the elastic modulus and Poisson's ratio of the cylinder liner are 140 GPa and 0.3, respectively. The elastic modulus and Poisson's ratio of the piston ring are 220 GPa and 0.3, respectively.

2.4. Two-scale wear model

When simulating the “zero-wear” of the cylinder liner, the plateau component wear is calculated on the local scale, and the valley component wear is calculated on the global scale. The wear calculation on both scales is governed by the Archard wear model. The local scale wear will affect the homogenized flow factors and contact stiffness, and the global wear will change the groove parameters. As a result, the lubrication behavior will be affected.

Archard's equation [17] postulates that wear volume is proportional to the load and sliding distance and inversely proportional to the hardness of the materials

$$\text{Vol} = K \frac{F_T s}{H} \quad (5)$$

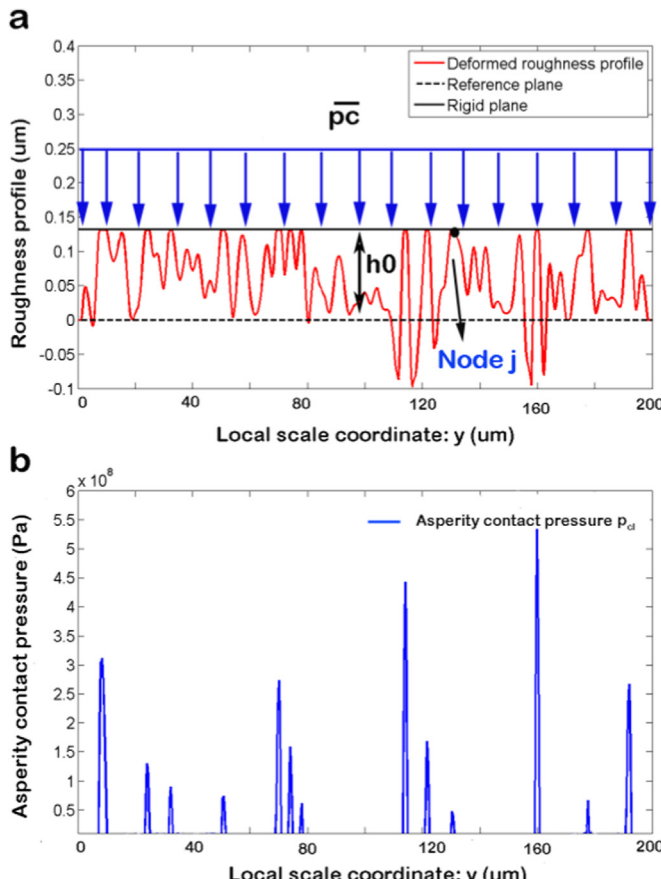


Fig. 4. (a) The deformed surface roughness profile and (b) the corresponding asperity contact pressure distribution under the applied load.

where Vol is the worn volume, F_T is the applied load, s is the sliding distance, H is the hardness of the soft material, and K is the dimensionless wear coefficient.

In order to be able to calculate the change in topography, Eq. (5) is rewritten to describe the wear depth at a certain point instead of wear volume.

$$h = kp_c s \quad (6)$$

where k is the dimensional wear coefficient $k = K/H$, p_c is the contact pressure, s is the sliding distance.

The wear depth at a certain point can be represented as the summation of the wear depth increment, thus, the equation can be rewritten as

$$\Delta h = kp_c \cdot \Delta s \quad (7)$$

2.4.1. Wear coefficient

The determination of wear coefficient is very crucial for the accurate simulation of the wear process. Molecular dynamics simulations show that as long as the wear mechanisms do not change, the Archard model is valid down to nanometric scale [37]. So, in this work, the wear calculations on both scales are based on Archard wear model. In addition, the wear coefficient is chosen to be the same on the local and global scales, i.e. $k_l = k_g = k$.

The wear coefficient can be determined by comparison of the wear depth predicted by the simulation to that measured in the experiments [5,38]. If the agreement is not satisfactory, then the wear coefficient can be modified until the simulated wear depth and the measured wear depth agree well. Thus, the wear coefficient of the system is obtained. The wear depth will be measured by means of tribological tests.

2.4.2. Wear calculation on the local scale

In case of local scale wear, the wear process of the plateau component within the entire stroke is reflected by simulating the wear process of a part of the plateau component with length of 1 mm along the sliding direction. The flow chart of wear calculation on the local scale is shown in Fig. 5(a).

At time $t_l = t_l^{(k)}$, the average contact pressure is obtained by averaging the instantaneous contact pressure over one cycle $\Delta\tau$.

$$\bar{p}_c(t_l^{(k)}) = \frac{1}{\Delta\tau W} \int_{t_l^{(k)}}^{t_l^{(k)} + \Delta\tau} \int_{-\frac{W}{2}}^{\frac{W}{2}} p_{cg}(x, \tau) dx d\tau \quad (8)$$

where $\bar{p}_c(t_l^{(k)})$ is the average contact pressure over one cycle, $\Delta\tau$ is the time interval of one cycle. In this case, $\Delta\tau = \frac{1}{6}s$. As shown in Fig. 2, $p_{cg}(x, \tau)$ is the contact pressure variation with time over one cycle on the global scale, which can be obtained by solving the homogenized mixed lubrication model. After the average contact pressure $\bar{p}_c(t_l^{(k)})$ is obtained, the asperity contact pressure distribution $p_{cl}(y, t_l^{(k)})$ within the length of the plateau can be calculated, as shown in Fig. 4(b). According to the Archard wear model, within one cycle, the piston ring moves across twice. Therefore, the wear depth increment at a node j on the plateau can be calculated as

$$\delta h_l(y_j, t_l^{(k)}) = 2k_l p_{cl}(y_j, t_l^{(k)}) W \quad (9)$$

where k_l is the wear coefficient on the local scale, δh_l is the wear depth increment over one cycle, W is the ring width. At time $t_l = t_l^{(k+1)}$,

$$h_l(y_j, t_l^{(k+1)}) = h_l(y_j, t_l^{(k)}) + \frac{\Delta t_l}{\Delta\tau} \delta h_l(y_j, t_l^{(k)}) \quad (10)$$

where $h_l(y_j, t_l^{(k+1)})$ and $h_l(y_j, t_l^{(k)})$ are the wear depth of the node j

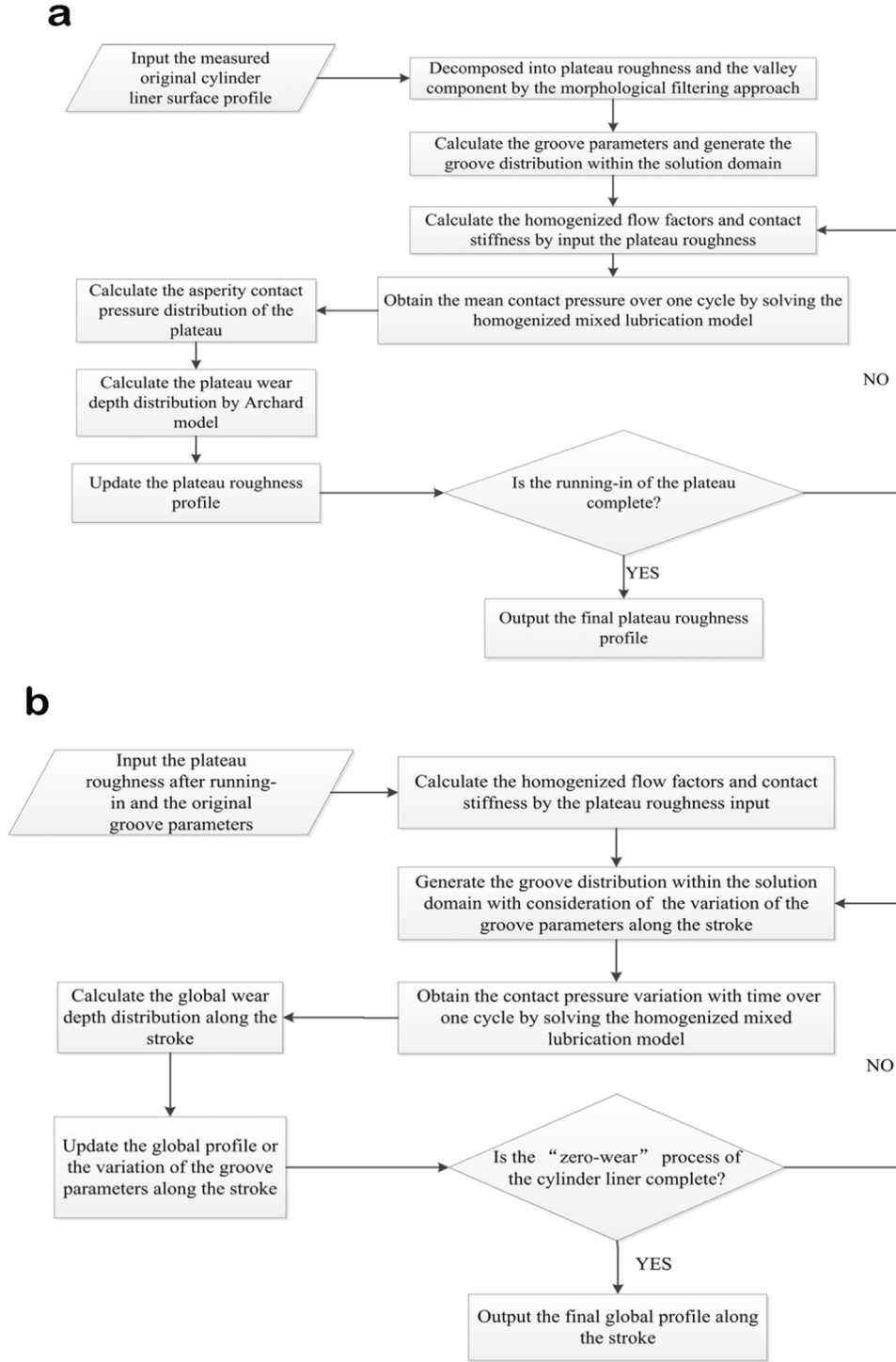


Fig. 5. (a) Flow chart of wear calculation on the local scale; (b) Flow-chart of wear calculation on the global scale.

on the plateau at time $t_l = t_l^{(k+1)}$ and $t_l = t_l^{(k)}$, respectively. Δt_l is the time step of wear calculation on the local scale.

In addition, during the running-in of plateau roughness, the plateau roughness profile is updated continuously. When the running-in process is complete, a steady-state condition is reached. The steady state is assumed to occur when the wear depth increment at two consecutive iterations fall below a specified tolerance value, i.e.,

$$|(h_l(j)^{\text{new}} - h_l(j)^{\text{old}}| < \epsilon \quad (11)$$

In this study, ϵ is set to be 5×10^{-9} m.

2.4.3. Wear calculation on the global scale

In case of wear calculation on the global scale, the differences of groove parameters and contact pressure at different positions of the stroke will be taken into consideration. The flow chart of wear calculation on the global scale is shown in Fig. 5 (b). To simplify the wear calculation on the global scale, it is assumed that the contact pressure distribution $p_{Cg}(x, \tau_j)$ does not change its profile when the piston ring is passing the node j , as shown in Fig. 2.

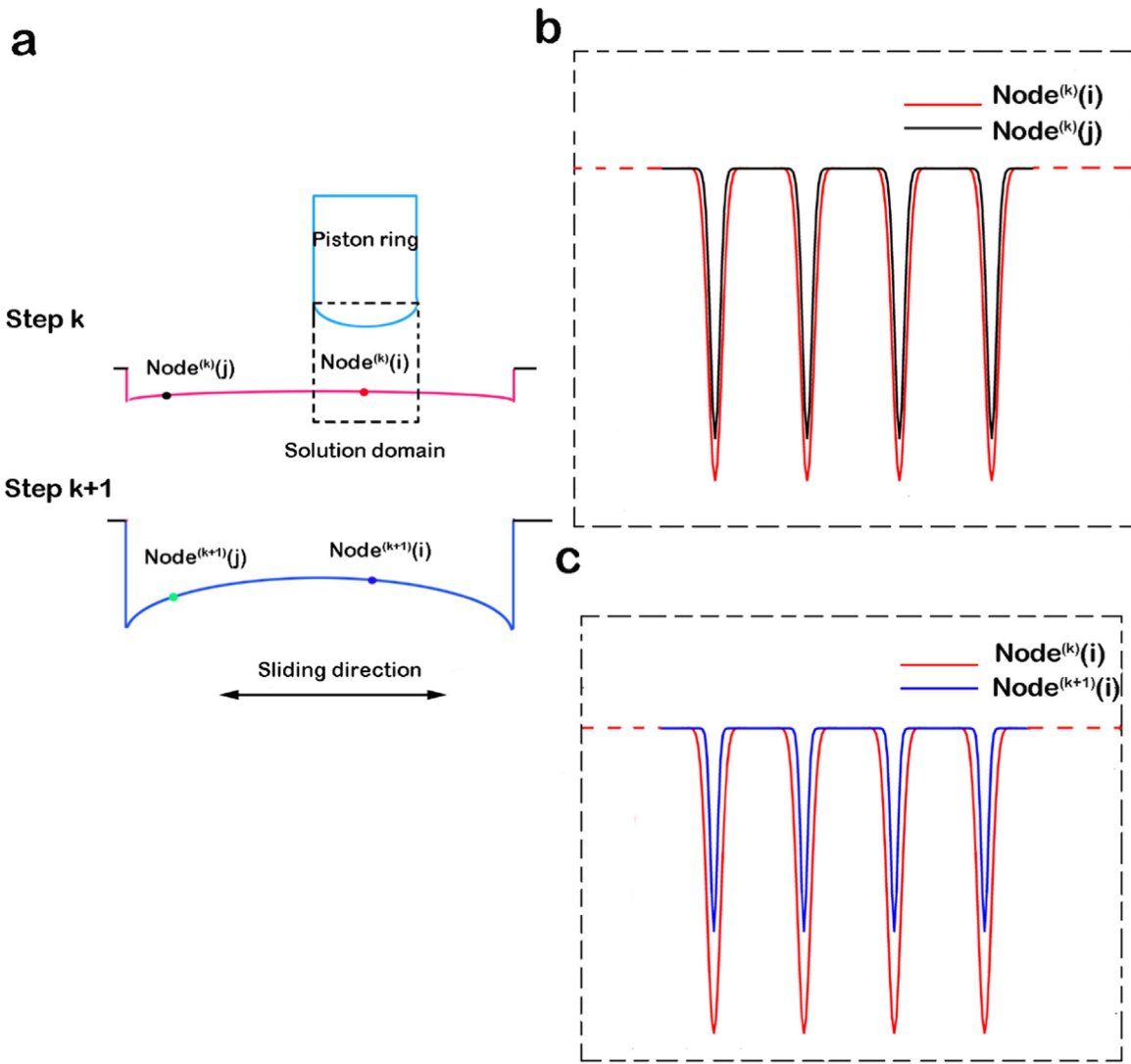


Fig. 6. A schematic diagram of the groove distribution updating within the solution domain on the global scale (i and j are the nodes on the stroke, k and $k + 1$ are the wear steps).

Furthermore, as the piston ring moves across twice within one cycle, thus, the wear depth increment can be calculated as

$$\delta h_g(s_j, t_g^{(k)}) = 2k_g \int_{-\frac{W}{2}}^{\frac{W}{2}} pc_g(x, \tau_j) dx \quad (12)$$

where k_g is the wear coefficient on the global scale, δh_g is the wear depth increment over one cycle, W is the ring width.

At time $t_g = t_g^{(k+1)}$, the wear depth of the node j on the cylinder liner can be calculated as

$$h_g(s_j, t_g^{(k+1)}) = h_g(s_j, t_g^{(k)}) + \frac{\Delta t_g}{\Delta \tau} \delta h_g(s_j, t_g^{(k)}) \quad (13)$$

where $h_g(s_j, t_g^{(k)})$ is the wear depth of the node j at time $t_g = t_g^{(k)}$. Δt_g is the time step of wear calculation on the global scale.

The calculations of the homogenized mixed lubrication model on different scales are different. In case of wear calculation on the local scale, the groove distribution within the solution domain remains unchanged when solving the homogenized mixed lubrication model. However, in case of wear calculation on the global scale, the groove parameters differ at different positions of the stroke due to the global scale wear. Therefore, when the piston passes a point i , the groove distribution should be updated.

For simplicity, it is assumed that the groove distribution within the ring width is uniform, and the groove near the point i will be repeated within the solution domain (ring width) as shown in Fig. 6(a). Fig. 6(b) shows the groove distribution differences when the piston ring passes different nodes on the stroke in the same time step. Fig. 6(c) shows the groove distribution differences when the piston ring passes the same node in different time steps. When the maximum wear depth at a node on the stroke reaches the mean groove depth of the original honed surface, the "zero-wear" process is complete, which also indicates the failure of the cylinder liner surface. Fig. 7 shows a schematic diagram of wear processes on two scales.

3. Experimental details

In order to validate the established wear model and obtain the wear coefficient, experiments are conducted in a sliding reciprocating rig. The samples are loaded with 200 N, the frequency is 6 Hz, and the stroke is 8 mm. The experiments are conducted at room temperature. The contact is lubricated with SAE30 oil. The experiments are recorded after 0.5, 1, 2 and 4 h test durations.

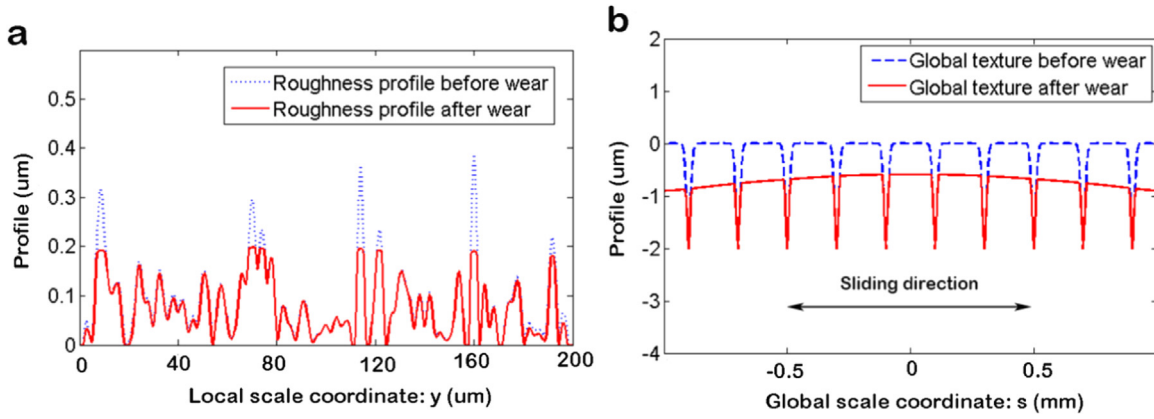


Fig. 7. A schematic image of wear on two scales.(a) the wear of the plateau on the local scale;(b) the wear of valley component on the global scale.

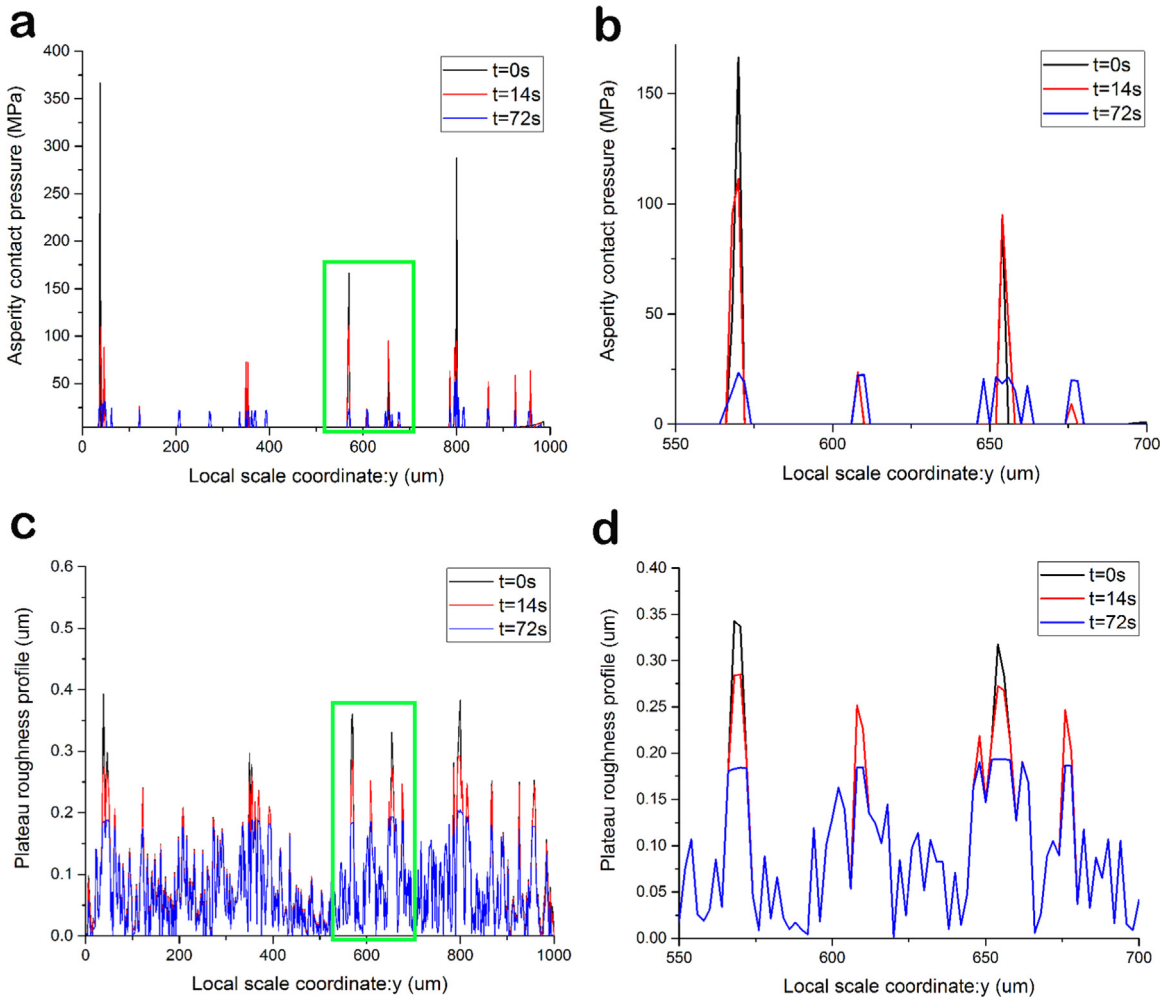


Fig. 8. Evolution of (a) asperity contact pressure distribution and (c) roughness profile during the running-in of the plateau component on the local scale ((b) and (d) are zoomed figure).

The piston ring is barrel-shaped, GDC coated, and 3.0-mm wide. The barrel height of the ring is 4 μm . The diameter of the ring is 115 mm. In order to promote circumferential conformity between the two specimens, a cylinder liner with a litter larger bore diameter of 125 mm was used. For the experiments, 15-mm-long sections of piston ring were cut from the same top compression ring. The

cylinder liner samples with size of 20-mm length and 30-mm width were cut from the same cylinder liner. Therefore, the liner samples have nearly the same roughness and material composition. Samples with surface defects are abandoned before experiments.

Surface topography measurements are carried out before and after each tribological test. All roughness measurements are

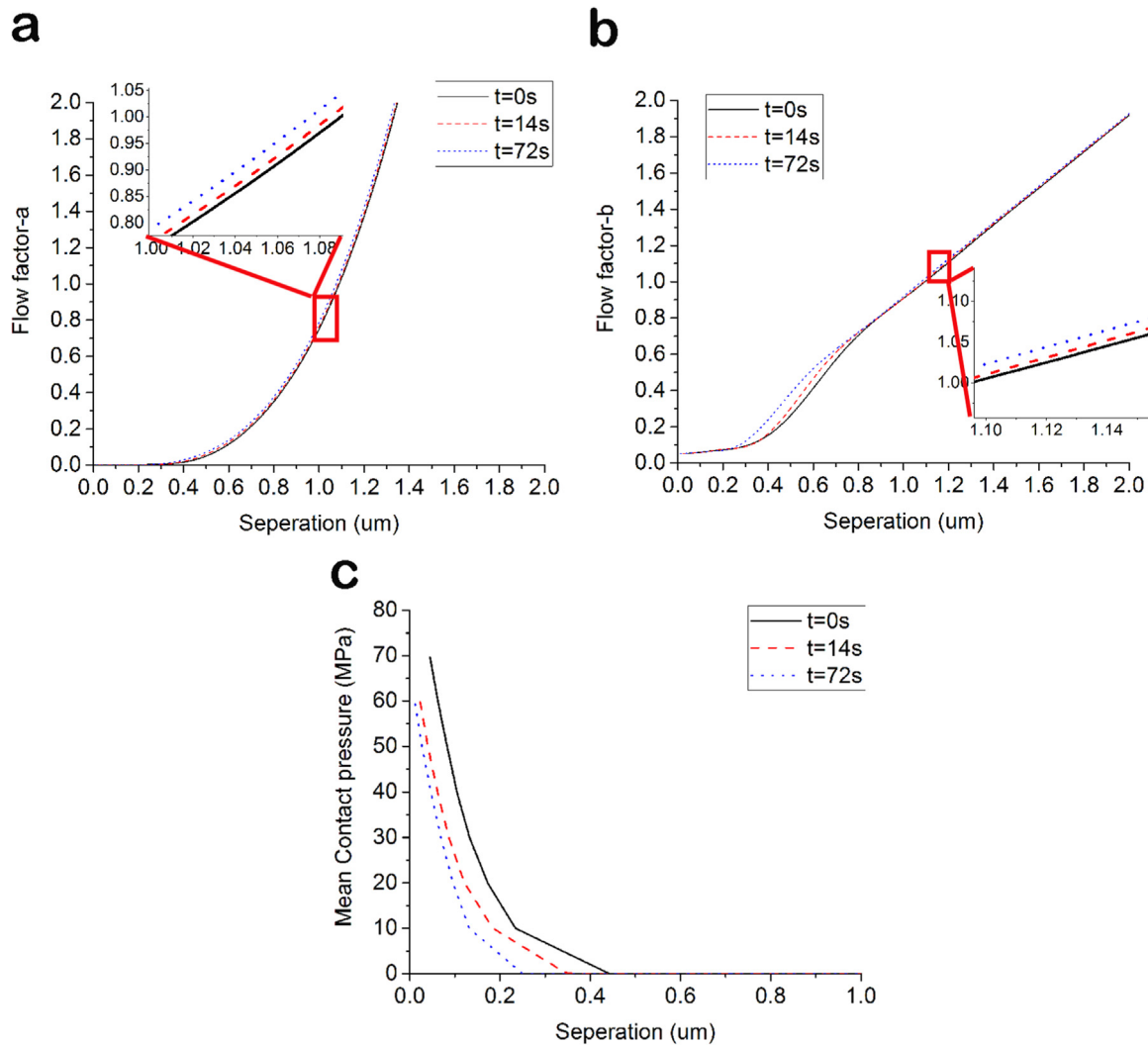


Fig. 9. Evolution of (a) the pressure flow factor a , (b) the shear flow factor b and (c) contact stiffness during the running-in of the plateau component.

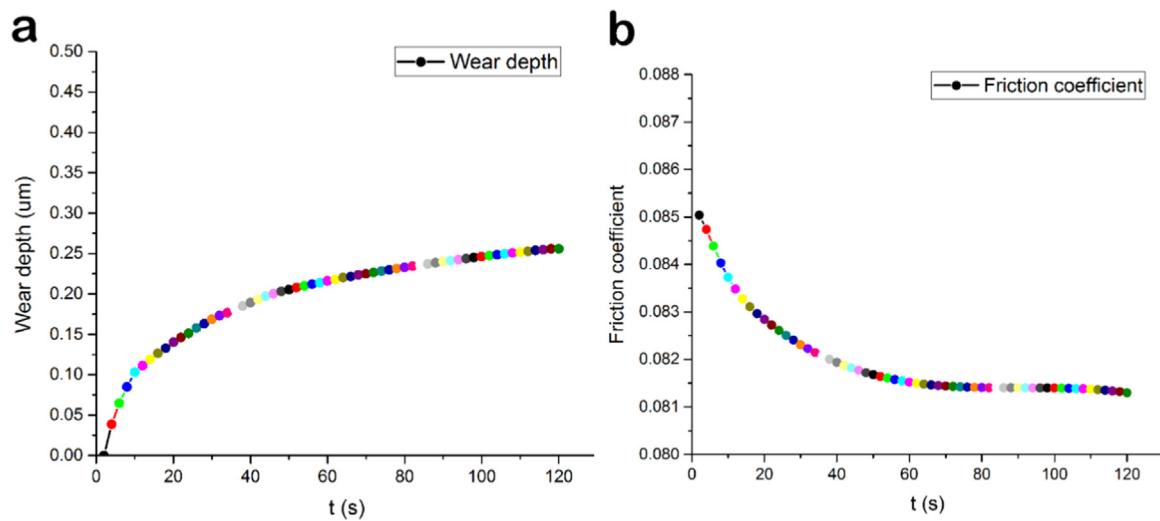


Fig. 10. Evolution of (a) wear depth and (b) friction coefficient during the running-in of the plateau component.

conducted with Contracer CV2100. Surface roughness measurements are limited to 2D profiles for practical reasons. All measurements in this study are conducted with a stylus sensor with a

tip radius of 5 μm and a normal load of 0.5 mN. The measurement speed is 0.5 mm/s. The length calibration is 0.5 μm, and the height calibration is 1 nm.

4. Results and discussion

4.1. 1 Experimental results

The original surface topography parameters of the cylinder liner and piston ring are measured. The measurements show that R_{pk} , R_k

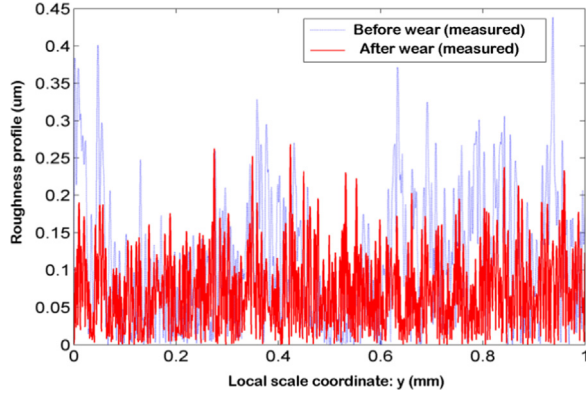


Fig. 11. The plateau roughness profiles decomposed from the measured cylinder liners before and after wear.

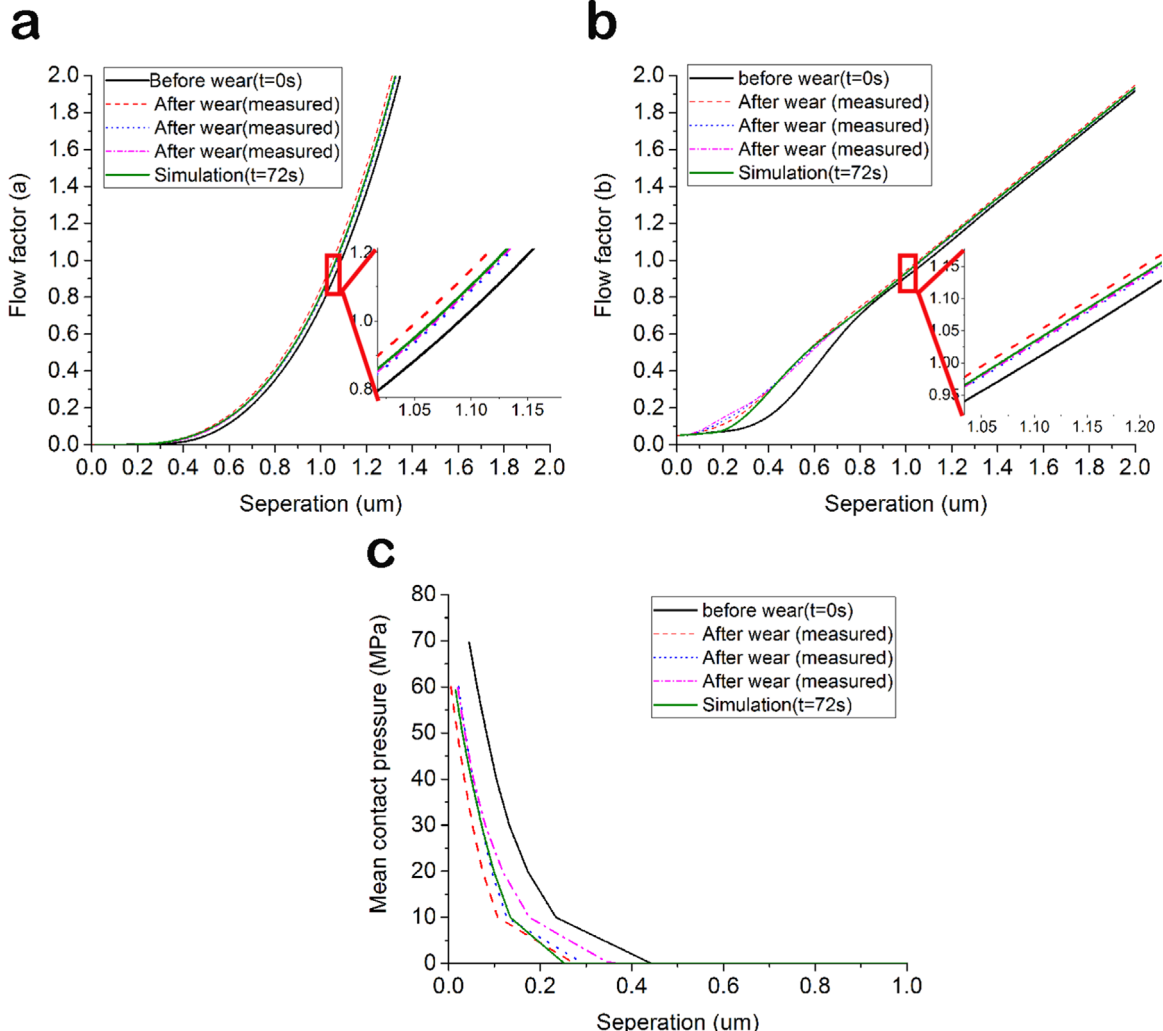


Fig. 12. Comparison between the homogenized flow factors and contact stiffness calculated from the predicted profile after running-in and the corresponding results calculated from the measured cylinder liner profiles with worn. The homogenized flow factors and contact stiffness calculated from the unworn surface are also shown in this figure.

and R_{vk} values of the cylinder liner are 0.195, 0.617 and 1.723 μm , respectively. Moreover, R_q value of the ring face is 0.048 μm , while R_q value of the cylinder liner surface is 0.608 μm . In comparison to the ring face, the cylinder liner surface topography is much rougher. Therefore, in this paper, the ring surface is assumed smooth, only the effects of the honed liner surface are considered.

The ring profiles measured before and after 4 h test duration show that the wear depth of the piston ring is less than 0.2 μm , and is very small, since the piston ring is GDC coated and has good wear resistance. So, in this study, the ring wear is ignored, and the study only focused on the “zero-wear” of the cylinder liner.

In this study, along the sliding direction, the surface profiles subjected to and not subjected to wear are measured simultaneously. The middle profile is subjected to wear, and the profiles at two ends are not subjected to wear. The average wear depth w_0 is equal to the P_t parameter (total profile height) of the whole profile minus the P_v parameter (maximum valley depth) of the middle profile [39,40]. The procedure was repeated 3–5 times for each sample. After obtaining the average wear depth, the final wear coefficient can be achieved by following the procedures as described in Section 2.4.1. The final wear coefficient for the piston ring-liner system is determined as $k_l = k_g = 8.1 \times 10^{-16} \text{ Pa}^{-1}$. The wear coefficient will be used to calculate both the local and global scale wear.

4.2. Simulation results on the local scale

In this section, evolution of the asperity contact pressure distribution and the plateau roughness profile with time due to local scale wear are firstly presented. Then, the effects of local scale wear on the changes of homogenized flow factors and contact stiffness are analyzed. Finally, the local scale wear model is validated by comparing the homogenized flow factors and contact stiffness calculated from the predicted profiles with the corresponding results calculated from the measured surfaces with worn.

Evolution of asperity contact pressure distribution and roughness profile during the running-in of the plateau component on the local scale are shown in Fig. 8(a) and (c), respectively. It can be seen that the roughness asperities are polished and the contact area is increased, thus leading to a lower and wider contact pressure distribution with time. Fig. 9 shows the evolution of homogenized flow factors and contact stiffness during running-in of the plateau component. As the asperities are polished during the running-in process, the pressure flow factor a and the shear flow factor b at a given separation both increased as shown in Fig. 9(a) and (b). Accordingly, the contact stiffness is decreased as shown in Fig. 9(c). Fig. 10 shows the evolution of wear depth and friction coefficient during the running-in of the plateau

component. Initially, the wear depth increases rapidly and reaches to a stable value during the running-in process. Accordingly, the friction coefficient decreases rapidly and reaches to a stable value. The duration of local scale wear is short. The reduction of friction coefficient at this stage is due to the polishing of plateau roughness asperities on the local scale, as shown in Fig. 8. The polishing of asperities will lead to the decrease of asperity contact pressure, thus, the asperity friction decreases a lot.

The plateau roughness profiles that decomposed from the cylinder liner samples with and without worn are shown in Fig. 11. The homogenized flow factors and contact stiffness calculated from the predicted profile after running-in are compared to the corresponding results calculated from the measured cylinder liner profiles with worn as depicted in Fig. 12. The homogenized flow factors and contact stiffness calculated from the surface measurement of the unworn cylinder liner are taken as the initial values. Other curves of homogenized flow factors and contact stiffness calculated from the measured surfaces with worn are also shown in this figure. The results show that the homogenized flow factors and contact stiffness calculated from the predicted profile after running-in are similar to the corresponding results calculated from the measured cylinder liner samples with worn, which indicates that the local scale wear model is effective.

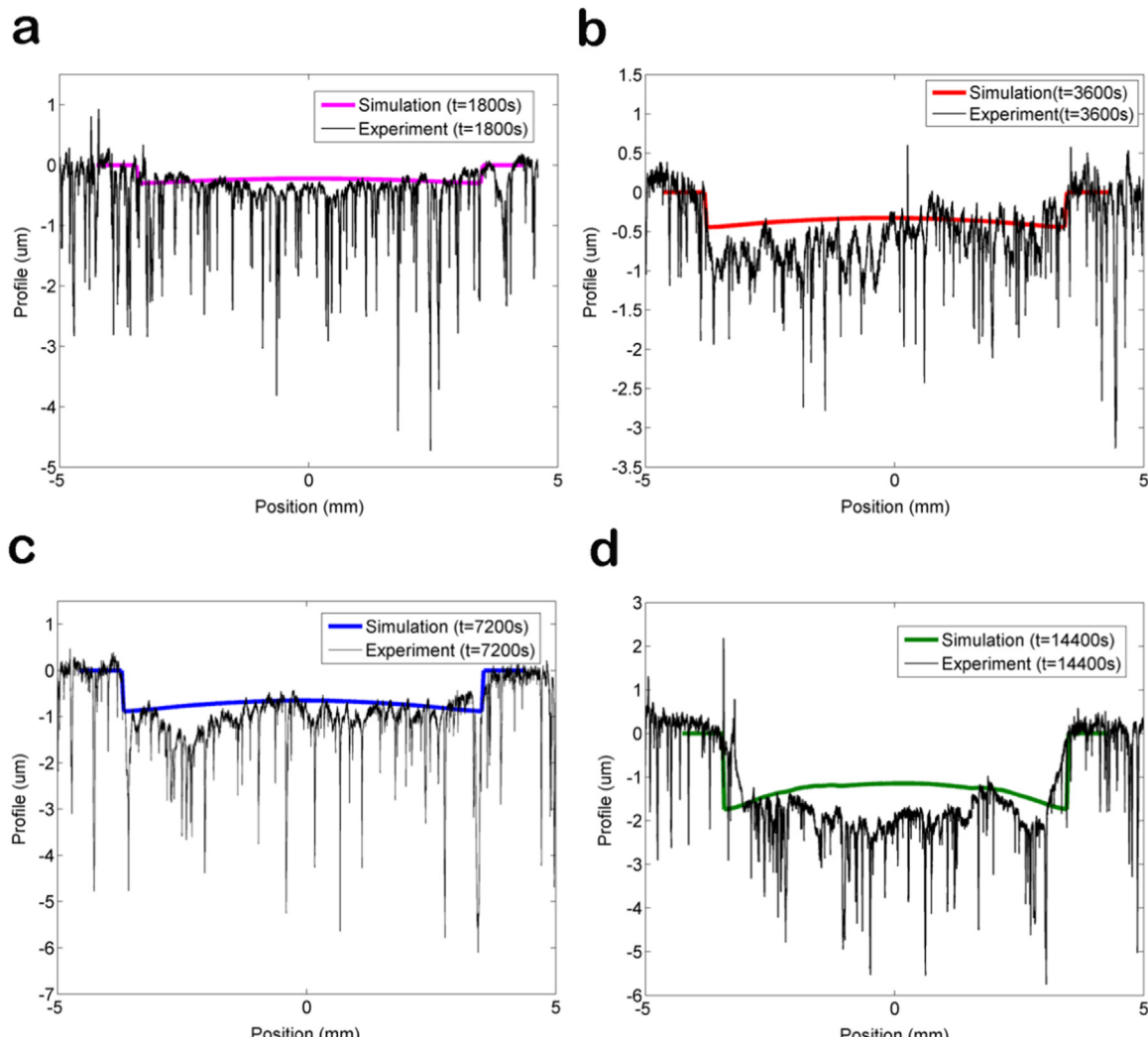


Fig. 13. Comparison of the predicted and experimental measured worn profiles along the sliding direction. (a): Test time: 1800 s; (b): Test time: 3600 s; (c): Test time: 7200 s; (d):Test time: 14400 s.

4.3. Simulation results on the global scale

Fig. 13 shows the comparison of the predicted and measured worn profiles along the sliding direction. The simulation results show that the wear depth increases with the increased test time. The simulated worn profiles indicate that the wear is strong near the edges, while in the middle part wear is relatively low. This can be attributed to that the hydrodynamic effect is not obvious near the edges with the low velocity, besides, the contact pressure is relative high, thus the wear is more severe. Similar trends are also observed in the experiments. The simulation results are shown to be in good agreement with the simulation results.

Fig. 14 shows the comparison between the predicted and measured friction coefficient and wear depth during the “zero-wear” process. As shown in **Fig. 14(a)**, after the rapid running-in process of the plateau component, the friction coefficient decreases gradually and slowly. During this stage, the reduction of friction is mainly due to the wear of the valley component on the global scale. Some deep and wide grooves will be gradually changed into shallow and fine grooves. The changed grooves will lead to the increased load carrying capacity, thus reducing the contact pressure. As a result, the friction is gradually reduced. The measured friction coefficient has a similar trend. The gradually decreasing of the friction coefficient during the test has also been

observed in other references [40,41]. **Fig. 14(b)** shows the comparison of the experimental measured and predicted wear depth during the “zero-wear” process. In the first few minutes, the wear rate is quite high due to the running-in of the plateaus on the local scale, and thereafter the wear rate gradually decreases as a result of the valley component wear on the global scale. It reveals that the wear model developed accurately capture the characteristics of the “zero-wear” of the cylinder liner with reasonable accuracy. **Fig. 14(c)** and **(d)** show the relative difference between the simulated and measured friction coefficient and wear depth, respectively. The approach to obtain the relative difference is their absolute difference divided by the measured value. The differences between the simulated and measured results can be attributed to three main reasons. Firstly, in our study, the piston ring-liner system is treated as a one-dimensional problem. The one-dimensional model has the advantages of simplicity, low computational effort and acceptable calculation precision which are beneficial for the study of the cylinder “zero-wear” process. However, the honed cylinder liner surface consists of cross-hatched texture and smooth plateau. The one-dimensional model cannot take into consideration the variation in the circumferential direction and the honing angle. Therefore, it is unable to fully predict the complex hydrodynamic phenomena. Secondly, in our experiments, in order to promote circumferential conformity between the piston ring

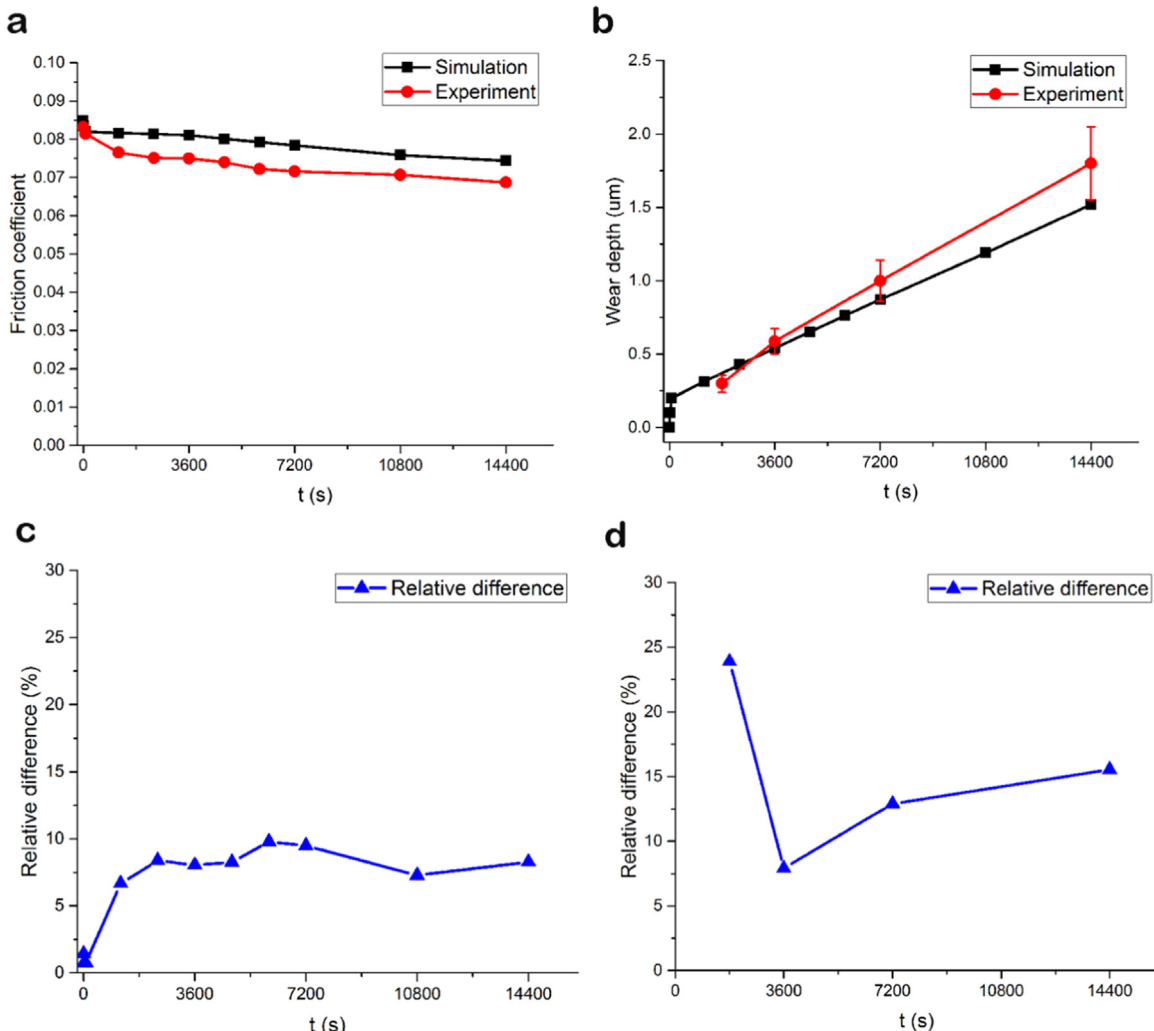


Fig. 14. (a) comparison of the predicted and measured friction coefficient over time; (b) comparison of the predicted and the experimental measured wear depth during the “zero-wear” process; (c) the relative difference of friction coefficient and (d) the relative difference of wear depth.

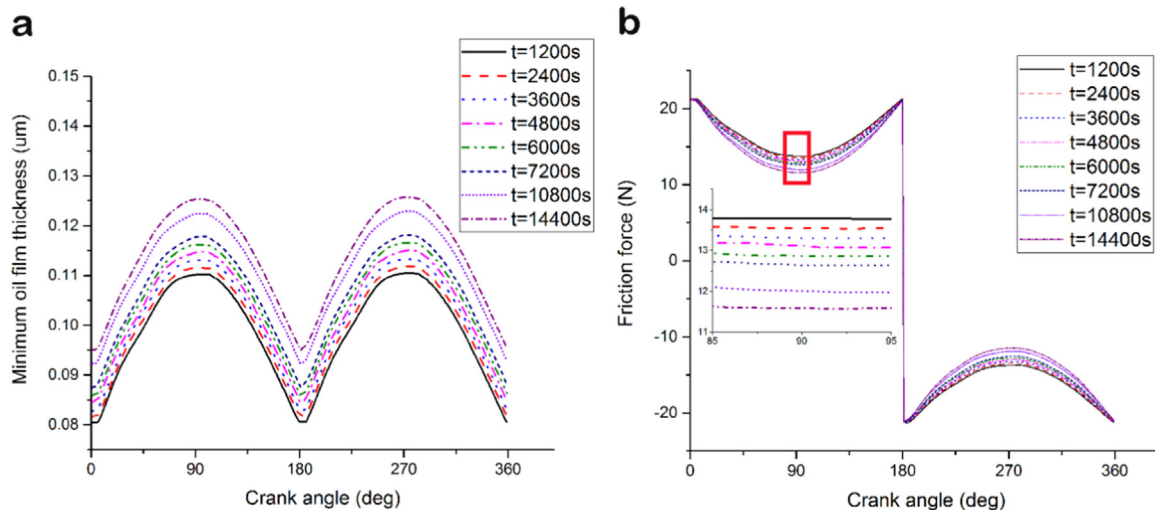


Fig. 15. Evolution of (a) minimum oil film thickness and (b) friction force over time.

sample and liner sample, the diameter of the cylinder liner sample is chosen to be greater than that of the piston ring sample. Therefore, the experimental condition is not exactly the same as the simulation condition. Thirdly, in our model, the piston ring is assumed to be smooth and the wear of piston ring is ignored. However, in the experiments, the surface topography of the piston ring will influence the friction and wear performance of the system to some extent.

Fig. 15 shows the variations of the predicted minimum oil film thickness and friction force with time. The minimum oil film thickness increases while the friction decreases due to the global scale wear.

5. Conclusions

In this paper, a two-scale homogenized mixed lubrication and wear model was established to study the cylinder “zero-wear” process. The mutual dependency of mixed lubrication and wear is involved in this study. Based on the Archard wear model, the “zero-wear” process of the cylinder liner is quantitatively investigated on two scales: on the local scale, considering the superficial plateau wear, and on the global scale, considering the valley component wear. The simulation results show that on the local scale, the wear of the plateaus will influence the homogenized flow factors and contact stiffness; on the global scale, the valley component wear will affect the lubrication properties. In addition, the model is verified by the reciprocating tests, which indicates that the developed model can well predict the “zero-wear” process of the cylinder liner. This paper focuses on the “zero-wear” of the cylinder liner, and the effect of the wear of the piston ring is neglected for the present, which can be coupled into the model in the future. This model provides an effective means to predict and improve the service life of the piston ring-liner system in an internal combustion engine.

Acknowledgements

The authors are most grateful to the National Natural Science Foundation of China (Grant No. 51375300, 51575342), the Research Project of State Key Laboratory of Mechanical System and Vibration (Grant No. MSVZD201401) for supporting this research.

References

- [1] P. Pawlus, J. Michalski, Simulation of cylinder ‘zero-wear’ process, *Wear* 266 (2009) 208–213.
- [2] Z. Krzyzak, P. Pawlus, ‘Zero-wear’ of piston skirt surface topography, *Wear* 260 (2006) 554–561.
- [3] T.S. Eyre, K.K. Dutta, F.A. Davis, Characterization and simulation of wear occurring in the cylinder bore of the internal combustion engine, *Tribol. Int.* 23 (1) (1990) 11–16.
- [4] Y.Z. Hu, D. Zhu, Full numerical solution to the mixed lubrication in point contacts, *ASME J. Tribol.* 122 (1) (2000) 1–9.
- [5] D. Zhu, A. Martini, W. Wang, et al., Simulation of sliding wear in mixed lubrication, *J. Tribol.* 129 (2007) 544.
- [6] Y. Hu, H. Cheng, T. Arai, Y. Kobayashi, S. Aoyama, Numerical simulation of piston ring in mixed lubrication – a nonaxisymmetrical analysis, *ASME J. Tribol.* 166 (1994) 470–478.
- [7] O. Akalin, G.M. Newaz, Piston ring–cylinder bore friction modeling in mixed lubrication regime: part I – analytical results, *ASME J. Tribol.* 123 (2001) 211–218.
- [8] N. Patir, H.S. Cheng, An average flow model for determining effects of three-dimensional roughness on partial hydrodynamic lubrication, *Trans. ASME* 100 (1978) 12–17.
- [9] J.A. Greenwood, J.B.P. Williamson, Contact of nominally flat surfaces, *Proc. R. Soc. Lond. A Math. Phys. Sci.* 295 (1966) 300–319.
- [10] J.A. Greenwood, J.H. Tripp, The contact of two nominally flat rough surfaces, *Proc. Inst. Mech. Eng.* 185 (48) (1970) 625–633.
- [11] A. Almqvist, J. Dasht, The homogenization process of the Reynolds equation describing compressible liquid flow, *Tribol. Int.* 39 (2006) 994–1002.
- [12] A. Almqvist, J. Fabricius, A. Spencer, et al., Similarities and differences between the flow factor method by patir and cheng and homogenization, *J. Tribology* 133 (2011) 031702.
- [13] P. Marklund, P.M. Lutg, A. Almqvist, et al., A mixed lubrication model incorporating measured surface topography. Part 1: theory of flow factors, *Proc. Inst. Mech. Eng. J: Eng. Tribol.* 224 (2010) 335–351.
- [14] P.M. Lutg, A. Almqvist, P. Marklund, et al., A mixed lubrication model incorporating measured surface topography. Part 2: roughness treatment, model validation, and simulation, *Proc. Inst. Mech. Eng. J: Eng. Tribol.* 224 (2010) 353–365.
- [15] M. Kane, B. Bou-Said, Comparison of homogenization and direct techniques for the treatment of roughness in incompressible lubrication, *J. Tribol.* 126 (2004) 733.
- [16] A. Spencer, A. Almqvist, R. Larsson, A semi-deterministic texture-roughness model of the piston ring–cylinder liner contact, *Proc. Inst. Mech. Eng. J: Eng. Tribol.* 225 (2011) 325–333.
- [17] J.F. Archard, Contact and rubbing of flat surfaces, *J. Appl. Phys.* 24 (1953) 981–988.
- [18] J. Lengiewicz, S. Stupkiewicz, Efficient model of evolution of wear in quasi-steady-state sliding contacts, *Wear* 303 (2013) 611–621.
- [19] L. Johansson, Numerical simulation of contact pressure evolution in fretting, *J. Tribology-Trans. ASME* 116 (1994) 247–254.
- [20] P. Pödra, S. Andersson, Simulating sliding wear with finite element method, *Tribol. Int.* 32 (2) (1999) 71–81.
- [21] I. Serre, M. Bonnet, R.M. Pradeilles-Duval, Modelling an abrasive wear experiment by the boundary element method, *C.R. l'Académie Sci. Paris Sér. II b* 329 (2001) 803–808.
- [22] G.K. Sfantis, M.H. Aliabadi, A boundary element formulation for three-dimensional sliding wear simulation, *Wear* 262 (2007) 672–683.

- [23] J. Andersson, A. Almqvist, R. Larsson, Numerical simulation of a wear experiment, *Wear* 271 (2011) 2947–2952.
- [24] J. Furustig, A. Almqvist, C.A. Bates, et al., A two scale mixed lubrication wearing-in model, applied to hydraulic motors, *Tribol. Int.* 90 (2015) 248–256.
- [25] E. Decencière, D. Jeulin, Morphological decomposition of the surface topography of an internal combustion engine cylinder to characterize wear, *Wear* 249 (5–6) (2001) 482–488.
- [26] Z. Dimkovski, C. Anderberg, R. Ohlsson, et al., Characterisation of worn cylinder liner surfaces by segmentation of honing and wear scratches, *Wear* 271 (2011) 548–552.
- [27] Z. Dimkovski, C. Anderberg, B.G. Rosén, et al., Quantification of the cold worked material inside the deep honing grooves on cylinder liner surfaces and its effect on wear, *Wear* 267 (2009) 2235–2242.
- [28] S. Mezghani, I. Demirci, H. Zahouani, et al., The effect of groove texture patterns on piston-ring pack friction, *Precis. Eng.* 36 (2012) 210–217.
- [29] P. Wall, J. Fabricius, E.K. Essel, et al., Reiterated homogenization applied in hydrodynamic lubrication, *Proc. Inst. Mech. Eng. J: J. Eng. Tribol.* 222 (2008) 827–841.
- [30] Y. Jeng, Theoretical analysis of piston-ring lubrication Part1-fully flooded lubrication, *Trib. Trans.* 35 (1992) 696–706.
- [31] Eduardo Tomanik, Modelling the hydrodynamic support of cylinder bore and piston rings with laser textured surfaces, *Tribol. Int.* 59 (2013) 90–96.
- [32] C.A.J. Roelandts, Correlation Aspects of the Viscosity-Temperature-Pressure Relationships of Lubricating Oils (Ph.D thesis), Technische Hogeschool te Delft, Netherlands, 1966.
- [33] D. Dowson, G.R. Higginson, *Elastohydrodynamic Lubrication: The Fundamentals of Roller and Gear Lubrication*, Pergamon, Oxford, 1966.
- [34] A. Ronen, I. Etsion, Y. Kligerman, Friction-reducing surface-texturing in reciprocating automotive components, *Tribol. Trans.* 44 (2001) 359–366.
- [35] V. Brizmer, Y. Kligerman, I. Etsion, A laser surface textured parallel thrust bearing, *Tribology Trans.* 46 (2003) 397–403.
- [36] A. Spencer, I. Dobryden, N. Almqvist, et al., The influence of afm and vsi techniques on the accurate calculation of tribological surface roughness parameters, *Tribol. Int.* 57 (2013) 242–250.
- [37] Vargonen Metin, Yang Yongjian, Huang Liping, Shi Yunfeng, Molecular simulation of tip wear in a single asperity sliding contact, *Wear* 307 (1–2) (2013) 150–154.
- [38] P. Bajpai, A. Kahraman, N.E. Anderson, A surface wear prediction methodology for parallel-axis gear pairs, *ASME J. Tribol.* 126 (2004) 597–605.
- [39] P. Pawlus, L. Galda, A. Dzierwa, et al., Abrasive wear resistance of textured steel rings, *Wear* 267 (2009) 1873–1882.
- [40] W. Grabon, P. Pawlus, J. Sep, Tribological characteristics of one-process and two-process cylinder liner honed surfaces under reciprocating sliding conditions, *Tribol. Int.* 43 (2010) 1882–1892.
- [41] E. Tomanik, Friction and wear bench tests of different engine liner surface finishes, *Tribol. Int.* 41 (2008) 1032–1038.